BUTTERWORTH HEINEMANN

0140-7007(95)00006-2

Int. J. Refrig. Vol. 18, No. 4, pp. 228–234, 1995
Copyright © 1995 Elsevier Science Ltd and IIR
Printed in Great Britain. All rights reserved
0140-7007/95/$10.00 + 0.00

Simple functions for fast calculations of selected thermodynamic properties of the ammonia–water system

J. Pátek and J. Klomfar
Institute of Thermomechanics, Academy of Sciences of the Czech Republic, Dolejškova 5, 18200 Prague 8, Czech Republic
Received 8 April 1993; revised 9 December 1994

A set of five equations describing vapour–liquid equilibrium properties of the ammonia–water system is presented. They are intended for use in the design of absorption processes. Using variable dependences of technical relevance the equations make it possible to avoid iterative evaluations. The equations were constructed by fitting critically assessed experimental data using simple functional forms. They cover the region within which absorption cycles commonly used operate most often. The enthalpy of the gas phase has been calculated in the ideal mixture approximation. The results are presented in the form of an enthalpy–concentration diagram.
(Keywords: refrigerants; ammonia–water mixture; equilibrium properties; absorption)

Fonctions simples pour calcul rapide de certaines propriétés thermodynamiques d'une installation ammoniac–eau

On présente un groupe de cinq équations décrivant les propriétés d'équilibre vapeur–liquide de l'installation ammoniac–eau. Ces équations sont destinées à la conception des processus d'absorption. Grâce à l'utilisation de dépendences variables liés à la technique, ces équations permettent d'éviter les calculs itératifs. L'utilisation des formes fonctionnelles simples a permis d'élaborer ces équations sur la base de données expérimentales qui avait été passées au crible. Elles couvrent la zone dans laquelle les cycles courants à absorption fonctionnent le plus souvent. On a calculé l'enthalpie de la phase gazeuse en supposant un mélange idéal. Les résultats sont présentés sous forme d'un diagramme enthalpie–concentration.

Nomenclature

a_i	Coefficients
h	Specific enthalpy (kJ kg^{-1})
M	Molar weight (kg mol^{-1})
N	Number of data points
p	Pressure (MPa)
T	Temperature (K)
x	Ammonia mole fraction in the liquid phase
y	Ammonia mole fraction in the gas phase
$\bar{z}$	Mean deviation
s	Systematic deviation
w	Ammonia mass fraction in the gas phase

Greek letters

σ	Root mean square deviation

Subscripts

A	Ammonia
g	Gas phase
i	Term of fitting polynomial
k	Experimental data point
l	Liquid phase
W	Water
0	Reference value

One of the global ecological problems – stratospheric ozone layer depletion – confronts science and technology with the need to search for environmentally acceptable substitutes for chlorofluorocarbons, which are responsible for the depletion. Besides a number of newly synthesized compounds, the binary system ammonia–water is under consideration again. The increasing attention paid to the ammonia–water mixture in the past few years arises from the possibility of substituting absorption systems for compression systems utilizing chlorofluorocarbons. In particular, absorption refrigerators and compression–absorption heat pumps are being considered for high-temperature applications. The natural character of this medium and its excellent thermodynamic properties equal out negative aspects, apparently overestimated in the past.

The design of processes and systems requires an easily programmable and time-efficient description of the

thermophysical properties of the working fluids employed. Thermodynamically consistent formulations of thermodynamic properties most often use temperature and density or temperature and pressure as input parameters[1]. The properties used for cycle, process and system calculations are required as functions of different combinations of independent variables. Moreover, the procedures calculating them are called many times per design point. Time-consuming iterations thus have to be executed. Iterative evaluations in the course of calculations can be avoided by using simplified thermodynamically inconsistent approximation equations in required variables valid with adequate accuracy within a range sufficient for the solution of a particular problem. Functions using variable dependences of technical relevance are especially useful in the case of fluids widely used in modern technological applications, such as steam[2,3]. They can be constructed by fitting either experimental data or values calculated from a thermodynamically consistent formulation of the medium properties.

In the present work, a set of equations describing the vapour–liquid equilibrium properties of the ammonia–water system necessary for absorption cycle design have been developed as an example of fast approximation functions. The set comprises the dependences needed for the construction of an enthalpy–concentration diagram: $T(p, x)$, $T(p, y)$, $y(p, x)$, $h_l(T, x)$, and $h_g(T, y)$. It contains the relationships needed most often. When the need for any further equation arises in a particular problem solution, the set can be easily completed.

Data selection

The following sources of vapour–liquid equilibrium data have been taken into consideration in the present work: Smolen *et al.*[4], Sassen *et al.*[5], Müller *et al.*[6], Rizvi and Heidemann[7], Guillevic *et al.*[8], Polak and Lu[9], Scatchard *et al.*[10], Clifford and Hunter[11], Wucherer[12], Mittasch *et al.*[13], Wilson[14], Postma[15], Mollier[16], and Perman[17,18]. All composition data have been converted to molar fractions, temperatures to K (ITS-90) and pressures to MPa.

A correlation of each experimental data set in itself was carried out at first to assess its precision and to identify contingent misprints. The T–p–x data of Mittasch *et al.*[13] and Wilson[14] proved to be considerably shifted in relation to results of other authors and therefore have been discarded. Similarly, the T–p–y data of Rizvi and Heidemann[7] have not been accepted, as their average systematic deviation from the correlation of data of other authors exceeds 4 K and their maximum absolute deviation amounts to 17 K.

The distribution of the experimental data points chosen for fitting over the plane of independent variables is shown for the relationship $T(p, x)$ in *Figures 1* and *2* and for $T(p, y)$ in *Figure 3*. The region of thermodynamic states covered by the proposed set of equations is constrained by the available data. The upper pressure limit is given by the data for the enthalpy of the liquid phase. Those of Zinner[19] ranging from −80 to 180 °C, i.e. from 0.002 MPa up to 2 MPa, have been used. We choose as the standard state of zero enthalpy for water, as well as for ammonia, the liquid water at the triple point.

The data of Scatchard *et al.*[10] used for correlation by

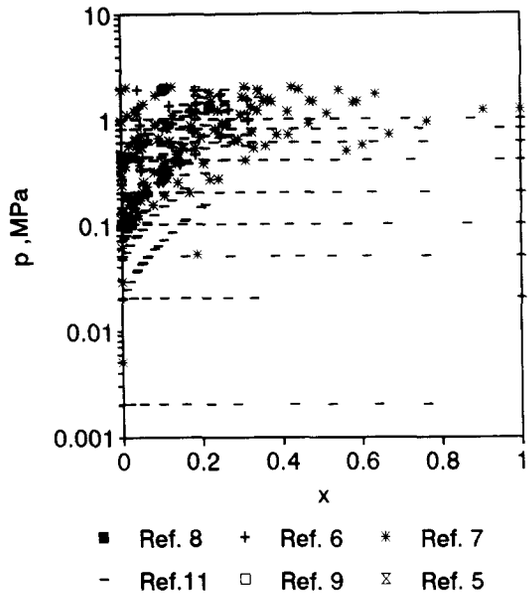

Figure 1 Distribution of the experimental data points for the function $T(p, x)$ over the plane of the independent variables p and x: Part I

Figure 1 *Répartition des points de mesure expérimentaux pour la fonction* (Tp, x) *en fonction des variables indépendantes* p *et* x; *premiere partie*

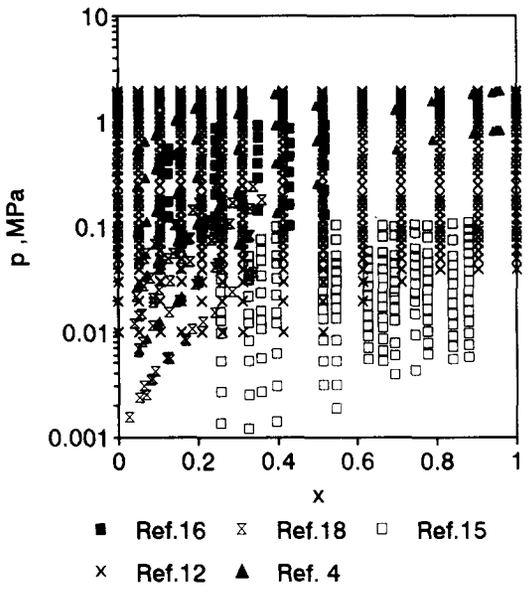

Figure 2 Distribution of the experimental data points for the function $T(p, x)$: Part II

Figure 2 *Répartition des points de mesure expérimentaux pour la fonction* (Tp, x); *deuxième partie*

Ziegler and Trepp[1] represent the data of Zinner[19] for enthalpy of the liquid phase and equilibrium T–p–x–y data of Wucherer[11] and Perman[18], smoothed using the Gibbs–Duhem relation to obtain consistent values. To avoid duplication, Scatchard's data have not been used in the present work.

Enthalpy of gaseous phase

Assuming the gas phase to be an ideal mixture of real components, the specific enthalpy $h_g(T, y)$ can be calculated from the enthalpy $h_A(T, p)$ and $h_W(T, p)$ of pure

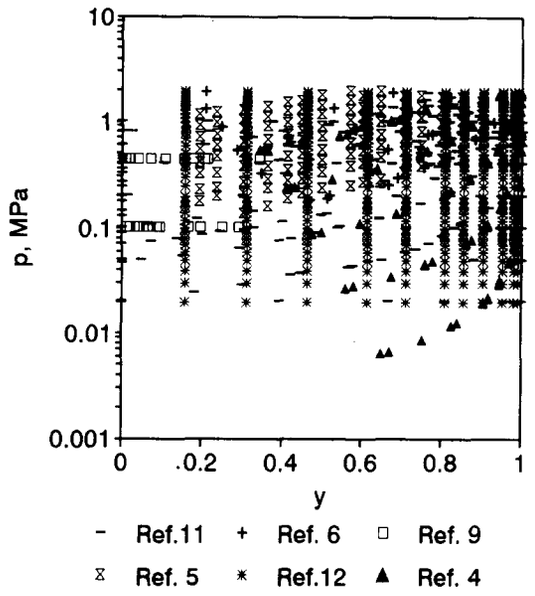

Figure 3 Distribution of the experimental data points for the function $T(p, y)$ over the plane of the independent variables p and y

Figure 3 *Répartition des points de mesure expérimentaux pour la fonction* (Tp, y) *en fonction des variables indépendantes* p *et* y

ammonia and water:

$$h_g(T, y) = (1 - w)h_W(T, p) + w \cdot h_A(T, p) \quad (1)$$

where

$$w = \frac{yM_A}{yM_A + (1 - y)M_W} \quad (2)$$

The value $p = p(T, y)$ corresponding to the phase equilibrium state has to be substituted in Equation (1) for pressure.

To compute the enthalpy of the system in the ideal mixture approach, the enthalpies of the pure components at the temperature and pressure of the mixture are required. While the temperatures and pressures in the region of interest relate to the states of the regular single-phase region of ammonia, they correspond to the hypothetical states of supersaturated vapour as regards water. Therefore, values of enthalpy extrapolated by means of a suitable equation of state from the single-phase region have to be employed as the best available approximation. The enthalpy of pure steam has been obtained from the formulation of Saul and Wagner[20] and that of pure ammonia from Haar and Gallagher[21].

Fitting procedure

The demands on the approximating functions were: a simple analytical form, fast evaluation, and a reasonable accuracy for industrial calculations. In general, an approximating function of a thermodynamic quantity z depending on variables u and v was sought in the form of a polynomial:

$$\zeta = \sum_i a_i \xi^{n_i} v^{m_i} \quad (3)$$

where

$$\zeta = Z(z, u, v); \qquad \xi = U(u, v); \qquad v = V(u, v) \quad (4)$$

are variables transformed by means of suitable functions U, V and Z. In this way the transformed relation is fitted by a polynomial in suitably chosen transformed variables. Then it is transformed back to the original variables.

A rational choice of the fitting polynomial terms was carried out by the step-wise regression method[20]. The reliability of any equation for the dependent variable z was verified by calculating the absolute deviation $\Delta z = z_{calc} - z_{exp}$ or the relative deviation $\delta z = \Delta z / z_{exp}$ for each data point, and the root mean square deviation σ, mean $\bar{z}$ and systematic deviation s for particular data sets. Average absolute deviations

$$\sigma = \left[\sum_k \frac{(\Delta z_k)^2}{N}\right]^{1/2}, \qquad \bar{z} = \sum_k \frac{|\Delta z_k|}{N}, \qquad s = \sum_k \frac{\Delta z_k}{N} \quad (5)$$

are relevant for temperature and enthalpy, for which only differences have a direct physical meaning. In the vicinity of the state where the enthalpy takes its zero value, the relative deviations provide no reasonable information. Concentration has an immediate physical meaning in itself and takes values over several orders. Therefore, average relative deviations are relevant for the $y(p, x)$ relation.

Resulting functional forms

The resulting functions best reproducing the selected experimental data show the following structure:

$$T(p, x) = T_0 \sum_i a_i (1 - x)^{m_i} \left[\ln\left(\frac{p_0}{p}\right)\right]^{n_i} \quad (6)$$

$$T(p, y) = T_0 \sum_i a_i (1 - y)^{m_i/4} \left[\ln\left(\frac{p_0}{p}\right)\right]^{n_i} \quad (7)$$

$$y(p, x) = 1 - \exp\left[\ln(1 - x) \sum_i a_i \left(\frac{p}{p_0}\right)^{m_i} x^{n_i/3}\right] \quad (8)$$

$$h_l(T, x) = h_0 \sum_i a_i \left(\frac{T}{T_0} - 1\right)^{m_i} x^{n_i} \quad (9)$$

$$h_g(T, y) = h_0 \sum_i a_i \left(1 - \frac{T}{T_0}\right)^{m_i} (1 - y)^{n_i/4} \quad (10)$$

The respective coefficients a_i of Equations (6)–(10) are given in *Tables 1–5*. The sources of the experimental data

Table 1 Exponents and coefficients of Equation (6)

Tableu 1 *Exposants et coefficients de l'équation (6)*

i	m_i	n_i	a_i
1	0	0	$+0.322\,302 \times 10^{1}$
2	0	1	$-0.384\,206 \times 10^{0}$
3	0	2	$+0.460\,965 \times 10^{-1}$
4	0	3	$-0.378\,945 \times 10^{-2}$
5	0	4	$+0.135\,610 \times 10^{-3}$
6	1	0	$+0.487\,755 \times 10^{0}$
7	1	1	$-0.120\,108 \times 10^{0}$
8	1	2	$+0.106\,154 \times 10^{-1}$
9	2	3	$-0.533\,589 \times 10^{-3}$
10	4	0	$+0.785\,041 \times 10^{1}$
11	5	0	$-0.115\,941 \times 10^{2}$
12	5	1	$-0.523\,150 \times 10^{-1}$
13	6	0	$+0.489\,596 \times 10^{1}$
14	13	1	$+0.421\,059 \times 10^{-1}$

$T_0 = 100$ K, $p_0 = 2$ MPa

Table 2 Exponents and coefficients of Equation (7)
Tableau 2 *Exposants et coefficients de l'equation (7)*

i	m_i	n_i	a_i
1	0	0	$+0.324004 \times 10^{1}$
2	0	1	-0.395920×10^{0}
3	0	2	$+0.435624 \times 10^{-1}$
4	0	3	-0.218943×10^{-2}
5	1	0	-0.143526×10^{1}
6	1	1	$+0.105256 \times 10^{1}$
7	1	2	-0.719281×10^{-1}
8	2	0	$+0.122362 \times 10^{2}$
9	2	1	-0.224368×10^{1}
10	3	0	-0.201780×10^{2}
11	3	1	$+0.110834 \times 10^{1}$
12	4	0	$+0.145399 \times 10^{2}$
13	4	2	$+0.644312 \times 10^{0}$
14	5	0	-0.221246×10^{1}
15	5	2	-0.756266×10^{0}
16	6	0	-0.135529×10^{1}
17	7	2	$+0.183541 \times 10^{0}$

$T_0 = 100$ K, $p_0 = 2$ MPa

Table 3 Exponents and coefficients of Equation (8)
Tableau 3 *Exposants et coefficients de l'equation (8)*

i	m_i	n_i	a_i
1	0	0	$+1.980220\,17 \times 10^{1}$
2	0	1	$-1.180926\,69 \times 10^{1}$
3	0	6	$+2.774799\,80 \times 10^{1}$
4	0	7	$-2.886342\,77 \times 10^{1}$
5	1	0	$-5.916166\,08 \times 10^{1}$
6	2	1	$+5.780913\,05 \times 10^{2}$
7	2	2	$-6.217367\,43 \times 10^{0}$
8	3	2	$-3.421984\,02 \times 10^{3}$
9	4	3	$+1.194031\,27 \times 10^{4}$
10	5	4	$-2.454137\,77 \times 10^{4}$
11	6	5	$+2.915918\,65 \times 10^{4}$
12	7	6	$-1.847822\,90 \times 10^{4}$
13	7	7	$+2.348194\,34 \times 10^{1}$
14	8	7	$+4.803106\,17 \times 10^{3}$

$p_0 = 2$ MPa

Table 4 Exponents and coefficients of Equation (9)
Tableau 4 *Exposants et coefficients de l'equation (9)*

i	m_i	n_i	a_i
1	0	1	-0.761080×10^{1}
2	0	4	$+0.256905 \times 10^{2}$
3	0	8	-0.247092×10^{3}
4	0	9	$+0.325952 \times 10^{3}$
5	0	12	-0.158854×10^{3}
6	0	14	$+0.619084 \times 10^{2}$
7	1	0	$+0.114314 \times 10^{2}$
8	1	1	$+0.118157 \times 10^{1}$
9	2	1	$+0.284179 \times 10^{1}$
10	3	3	$+0.741609 \times 10^{1}$
11	5	3	$+0.891844 \times 10^{3}$
12	5	4	-0.161309×10^{4}
13	5	5	$+0.622106 \times 10^{3}$
14	6	2	-0.207588×10^{3}
15	6	4	-0.687393×10^{1}
16	8	0	$+0.350716 \times 10^{1}$

$h_0 = 100$ kJ kg^{-1}, $T_0 = 273.16$ K

used for the correlation, together with the average deviations of the particular data sets from the correlation equation, and with bands of absolute or relative deviations are summarized in *Tables 6–8*. These

Table 5 Exponents and coefficients of Equation (10)
Tableau 5 *Exposants et coefficients de l'equation (10)*

i	m_i	n_i	a_i
1	0	0	$+0.128827 \times 10^{1}$
2	1	0	$+0.125247 \times 10^{0}$
3	2	0	-0.208748×10^{1}
4	3	0	$+0.217696 \times 10^{1}$
5	0	2	$+0.235687 \times 10^{1}$
6	1	2	-0.886987×10^{1}
7	2	2	$+0.102635 \times 10^{2}$
8	3	2	-0.237440×10^{1}
9	0	3	-0.670515×10^{1}
10	1	3	$+0.164508 \times 10^{2}$
11	2	3	-0.936849×10^{1}
12	0	4	$+0.842254 \times 10^{1}$
13	1	4	-0.858807×10^{1}
14	0	5	-0.277049×10^{1}
15	4	6	-0.961248×10^{0}
16	2	7	$+0.988009 \times 10^{0}$
17	1	10	$+0.308482 \times 10^{0}$

$h_0 = 1000$ kJ kg^{-1}, $T_0 = 324$ K

Table 6 Average deviations and bands of deviations of experimental data from Equation (6)
Tableau 6 *Ecarts moyens et fourchettes des écarts des données expérimentales de l'équation (6)*

Ref.	N	σ (K)	s (K)	$\bar{z}$ (K)	$\Delta y_{min} - \Delta y_{max}$ (K)
4	191	0.31	0.02	0.25	−1.1–0.7
5	4	1.90	1.80	1.80	0.9–2.4
6	29	0.84	−0.40	0.65	−2.2–1.6
7	105	1.70	0.80	1.40	−4.6–5.2
8	3	2.60	2.00	2.00	1.1–4.4
9	23	0.32	0.04	0.28	−1.0–0.4
11	241	0.70	−0.20	0.48	−3.1–3.0
12	490	0.48	0.01	0.40	−1.4–1.5
15	160	0.41	−0.20	0.33	−0.9–0.9
16	34	0.45	−0.20	0.33	−1.0–0.1
18	75	0.73	0.07	0.50	−2.6–2.4
Total	1365	0.72	0.00	0.45	−4.6–5.2

Table 7 Average deviations and bands of deviations of experimental data from Equation (7)
Tableau 7 *Ecarts moyens et fourchettes des écarts des données expérimentales de l'équation (7)*

Ref.	N	σ (K)	s (K)	$\bar{z}$ (K)	$\Delta y_{min} - \Delta y_{max}$ (K)
4	91	0.87	−0.43	0.73	−2.1–0.9
5	122	2.61	0.50	2.20	−4.5–5.9
6	29	1.70	0.34	1.30	−3.0–3.8
9	23	0.42	0.17	0.32	−1.3–0.6
11	191	1.50	−0.06	1.00	−7.0–3.5
12	378	0.84	−0.01	0.67	−2.0–2.7
Total	834	1.34	0.00	0.94	−7.0–5.9

Table 8 Average deviations and bands of deviations of experimental data from Equation (8)
Tableau 8 *Ecarts moyens et fourchettes des écarts des données expérimentales de l'équation (8)*

Ref.	N	σ (%)	s (%)	$\bar{z}$ (%)	$\Delta y_{min} - \Delta y_{max}$ (%)
4	156	0.72	−0.38	0.38	−2.6–0.3
6	24	1.80	1.00	1.30	−1.1–5.2
11	122	1.80	0.46	1.30	−6.7–5.4
12	177	0.48	−0.06	0.31	−2.1–1.5
Total	479	1.10	0.03	0.63	−6.7–5.4

deviations enable one to estimate the accuracy of the correlation. The precision of a particular set of data is evident from its band of deviations. Systematic deviations provide an idea of how the particular set is shifted as a whole with respect to the common average values given by the resultant function.

Equation (6) reproduces the $T(p, x)$ relation over the full concentration range from about 0.002 MPa to 2 MPa in pressures (see *Table 6* and *Figures 1* and *2*). An idea of the accuracy of this function is given by the fact that the absolute deviations of 95% of the fitted points are less than 1.5 K. Similarly, the range of use of Equation (7) for $T(p, y)$ is from 0.02 MPa to 2 MPa (*Table 7* and *Figure 3*); 95% of the fitted points are included in the ± 2 K absolute deviations band. The wider band of deviations of $T(p, y)$ is an evidence of greater difficulty encountered in measuring vapour composition. For comparison with independent formulation of the properties of the ammonia–water system, differences of data calculated from Equations (6) and (7) from those given by the formulation of Ziegler and Trepp[1] are presented in *Figures 4* and *5*.

To obtain a simple functional form for the $y(p, x)$ relation, its region of validity has to be curtailed to ammonia molar fractions in the liquid phase greater than 0.05 and pressures above 0.05 MPa. However, this limitation is not very onerous, since on the low-temperature side of refrigeration systems a pressure above

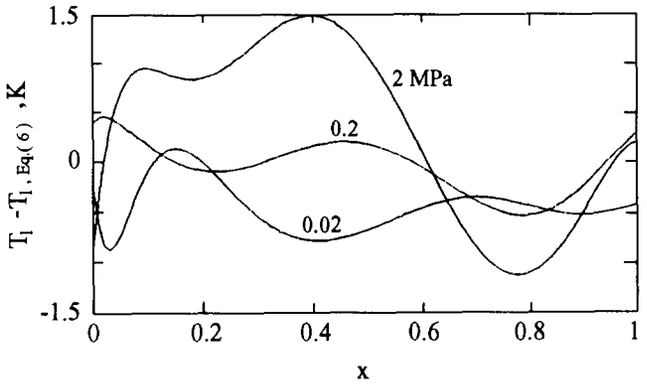

Figure 4 Comparison of $T(p, x)$ data collected from Equation (6) with the formulation of Ziegler and Trepp[1]

Figure 4 *Comparaison des données* T(p, x) *calculées à partir de l'equation (6) avec la formulation de Ziegler et Trepp*[1]

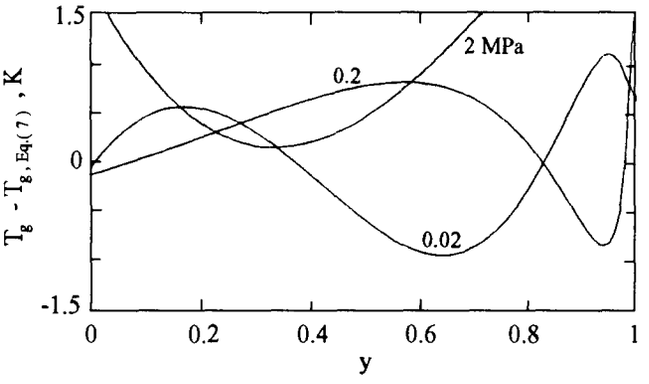

Figure 5 Comparison of $T(p, y)$ data calculated from Equation (7) with the formulation of Ziegler and Trepp[1]

Figure 4 *Comparaison des données* T(p, y) *calculées à partir de l'equation (7) avec la formulation de Ziegler et Trepp*[1]

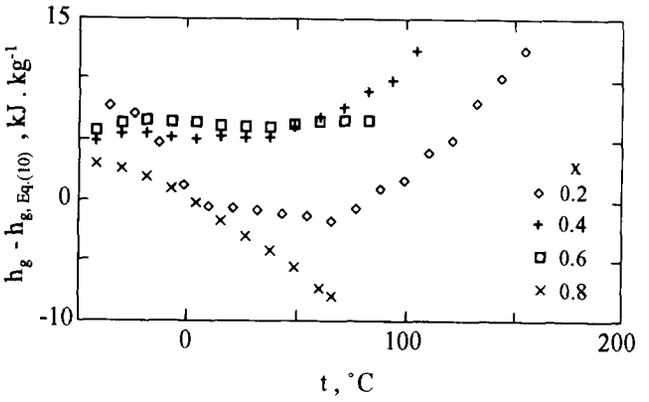

Figure 6 Comparison of gas-phase enthalpy calculated from Equation (10) along selected isopleths x = const. with data published by Scatchard *et al.*[10]

Figure 6 *Comparaison de l'enthalpie de la phase gazeuse calculée à partir de l'équation (10), le long de certaines lignes isoplethes choisies (x = const.), avec des données publiées par Scatchard* et al.

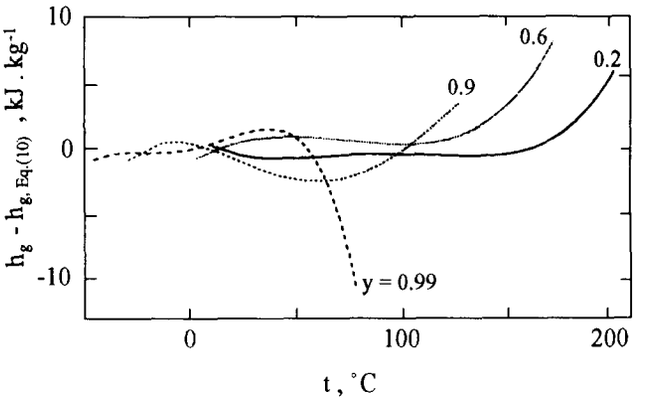

Figure 7 Comparison of $h_g(T, y)$ data calculated from Equation (10) with the formulation of Ziegler and Trepp[1] on four selected isopleths y = const.

Figure 7 *Comparaison des données* h_g(T, y), *calculées à partir de l'équation (10) avec la formulation de Ziegler et Trepp sur quatre lignes isoplethes choisies (y = const.)*

atmospheric is preferred to avoid leakage of air into them, and to increase the capacity of the cycle. The numerical consistency of the equations for $T(p, x)$, $T(p, y)$ and $y(p, x)$ has been checked and found to be better than 1% in y for x above 0.2 and not worse than 5% for concentrations less than 0.2.

Equation (9) reproduces the data of Zinner[19] for the specific enthalpy of the liquid phase with root mean square deviation 0.9 kJ kg^{-1}; deviations of the fitted values from the equation are enclosed within the band from -2.1 kJ kg^{-1} to 2.5 kJ kg^{-1}.

Values of enthalpy of the gas phase have been computed from Equation (1) on a grid of suitably selected points and fitted using the functional form (Equation (10)). The resultant values have been compared with those published by Scatchard *et al.*[10] (*Figure 6*) and those calculated from the formulation of Ziegler and Trepp[1] (*Figure 7*). In both cases the differences are less than 1% over the entire region from 0.02 to 2 MPa.

The part of the resultant enthalpy–concentration diagram concerning the gas phase is shown in *Figure 8* and that of the liquid phase in *Figure 9*, bounded from below by the melting line as measured by Postma[15]. The

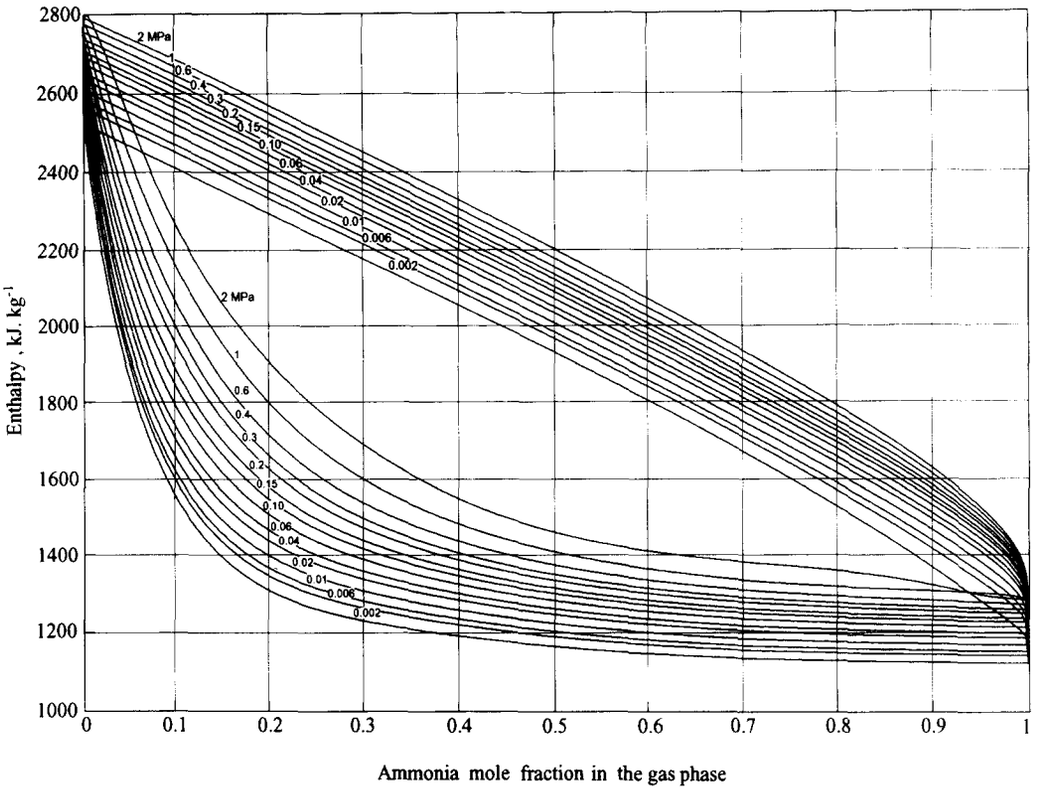

Figure 8 Enthalpy–concentration diagram, gaseous phase

Figure 8 *Diagramme enthalpie–concentration; partie consacrée à la phase gazeuse*

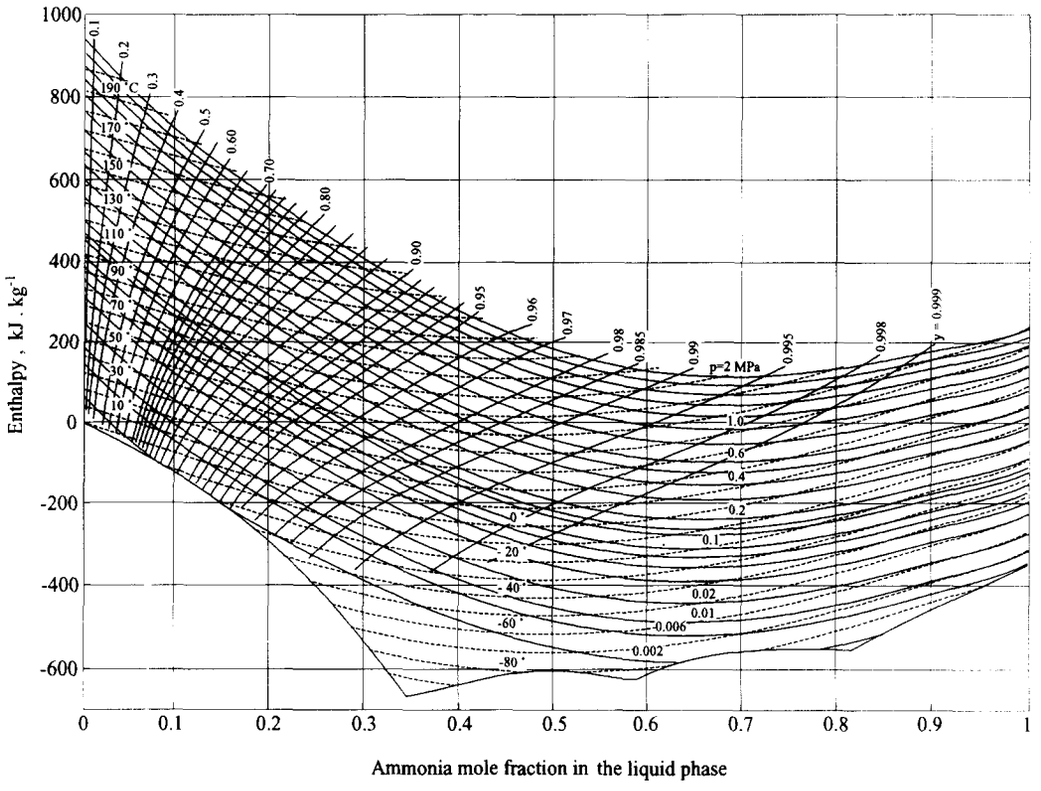

Figure 9 Enthalpy–concentration diagram, liquid phase

Figure 9 *Diagramme enthalpie–concentration; partie consacrée à la phase liquide*

bubble lines $h_g(p, x)$ in *Figure 8* are constructed as a composite function $h_g(T(p, x), y(p, x))$. Therefore, the validity of the $h_g(p, x)$ relation is limited through the $y(p, x)$ relation to $x > 0.05$. Slight irregularities in derivatives shown by the liquid isotherms and isobars for $x > 0.8$ should be ascribed to the fitted data as they are reproduced with deviation not exceeding 1.6 kJ kg^{-1} in this region.

The enthalpy of saturated ammonia liquid shows a maximum near 2 MPa. This is why all isobars corresponding to higher pressures intersect those of lower pressures, as seen on the isobar for 2 MPa in *Figure 8*.

Conclusions

The suitable general functional forms presented in this work, once found, are applicable to any new experimental data; fitting of the respective coefficients only is required. The accuracy of the equations follows from the deviations of the experimental data points used for fitting given in *Tables 6–8*. The root mean square deviation 0.7 K for $T(p, x)$ corresponds to a mean probable error of ± 0.5 K. Similarly, estimation of the mean probable error for the $T(p, y)$ relation gives the value ± 0.8 K. The overall accuracy of the specific enthalpy of the liquid phase given by uncertainty in Zinner's data and by the approximation amounts to 4 kJ kg^{-1}. Thus when $h_l(T, x)$ and $h_g(T, y)$ are combined with the relationships $T(p, y)$ and $T(p, x)$ or $y(p, x)$ they give differences in enthalpy between the liquid and gas phases with accuracy better than 1%, i.e. about 10 kJ kg^{-1}.

As well as avoiding iterative calculations, the merit of the fast approximation functions consists in their simplicity, which facilitates their incorporation in any computer code. Nevertheless, some care is needed when using them, to ensure the convergence of iterative engineering calculations (e.g. in optimization procedures), as the accuracy required depends on the nature of the calculations.

The equations presented can also be used to calculate initial values for a consistent formulation. When employed in this alternative way, they provide a substantial reduction in the number of iterations.

References

1 **Ziegler, B., Trepp, Ch.** Equation of state for ammonia–water mixtures *Int J Refrig* (1984) **7** 101–106

2 **Schiebener, P., Straub, J.** Fast evaluation algorithms for properties of state exemplified with ordinary water substance *Proc 11th Conference on the Properties of Steam* Prague (1990) 271–277

3 **Meyer-Pitroff, R.** What power industry expects of steam research *Proc 10th International Conference on the Properties of Steam* Moscow (1984) 57–69

4 **Smolen, T. M., Manley, D. B., Poling, B. E.** Vapor–liquid equilibrium data for the NH_3–H_2O system and its description with a modified cubic equation *J Chem Eng Data* (1991) **36** 202–208

5 **Sassen, C. L., Kwartel, R. A. C., van der Kooi, H. J., de Swaan Arons, J.** Vapor–liquid equilibria for the system ammonia + water up to the critical region *J Chem Eng Data* (1990) **35** 140–144

6 **Müller, G., Bender, E., Maurer, G.** Das Dampf-Flüssigkeits-gleichgewicht des ternären Systems Ammoniak–Kohlendioxid–Wasser bei hohen Wassergehalten im Bereich zwischen 373 und 473 Kelvin *Ber Bunsenges Phys Chem* (1988) **92** 148–160

7 **Rizvi, S. S. H., Heidemann, R. A.** Vapor–liquid equilibria in the ammonia–water system *J Chem Eng Data* (1987) **32** 183–191

8 **Guillevic, J. L., Richon, D., Renon, H.** Vapor–liquid equilibrium data for the binary system water–ammonia at 403.1, 453.1 and 503.1 K up to 7 MPa *J Chem Eng Data* (1985) **30** 332–335

9 **Polak, J., Lu, B. C. Y.** Vapor–liquid equilibria in system ammonia–water at 14.69 and 65 Psia *J Chem Eng Data* (1975) **20** 182–183

10 **Scatchard, G., Epstein, L. F., Warburton, J., Cody, P. J.** Thermodynamic properties – saturated liquid and vapor of ammonia–water mixtures *Refrig Eng* (1947) **53** 413–452

11 **Clifford, I. L., Hunter, E.** The system ammonia–water at temperatures up to 150 °C and at pressures up to twenty atmospheres *J Phys Chem* (1933) **37** 101–118

12 **Wucherer, J.** Messung von Druck, Temperatur und Zusammensetzung der flüssigen und dampfförmigen Phase von Ammoniak–Wassergemischen *Z Ges Kälte-Ind* (1932) **39** 97–104, 136–140

13 **Mittasch, A., Kuss, E., Schleuter, H.** Dichten und Dampfdrücke von wäßrigen Ammoniaklösungen und von flüssigem Stickstofftetroxyd für das Temperaturgebiet 0° bis 60° *Z Anorg Allg Chem* (1926) **159** 1–35

14 **Wilson, T. A.** Properties of aqua-ammonia. Part 1. The total vapor pressures *Refrig Eng* (1924) **10** 248–252

15 **Postma, S.** Le système ammoniaque–eau *Recl Trav Chim* (1920) **39** 515–536

16 **Mollier, H.** Dampfdruck von wässrigen Ammoniaklösungen *Z Ver Deutsch Ing* (1908) **52** 1315–1320

17 **Perman, E. P.** Vapour pressure of aqueous ammonia solution, Part I *J Chem Soc (Lond)* (1901) **79** 718–725

18 **Perman, E. P.** Vapour pressure of aqueous ammonia solution, Part II *J Chem Soc (Lond)* (1903) **83** 1168–1184

19 **Zinner, K.** Wärmetönung beim Mischen von Ammoniak und Wasser in Abhängigkeit von Zusammensetzung und Temperatur *Z Ges Kalte-Ind* (1934) **41** 21–29

20 **Saul, A., Wagner, W.** A fundamental equation for water covering the range from the melting line to 1273 K at pressures up to 25000 MPa *J Phys Chem Ref Data* (1989) **18** 1537–1564

21 **Haar, L., Gallagher, J. S.** Thermodynamic properties of ammonia *J Phys Chem Ref Data* (1978) **7** 635–792

22 **de Reuck, K. M., Armstrong, B.** A method of correlation using a search procedure based on step-wise least-square technique, and its application to an equation of state for propylene *Cryogenics* (1979) **19** 505